Original Article

Prognostic implications of cellular senescence in resected non-small cell lung cancer

Andreas Domen[1,2]^, Christophe Deben[1]^, Ines De Pauw[1]^, Christophe Hermans[1,3], Hilde Lambrechts[1], Jasper Verswyvel[1]^, Vasiliki Siozopoulou[1,3]^, Patrick Pauwels[1,3]^, Marco Demaria[4]^, Mick van de Wiel[5], Annelies Janssens[5]^, Jeroen M. H. Hendriks[6]^, Paul Van Schil[6]^, Jan B. Vermorken[1,2]^, Timon Vandamme[1,2]^, Hans Prenen[1,2]^, Marc Peeters[1,2]^, Filip Lardon[1]^, An Wouters[1]^

[1]Center for Oncological Research (CORE), Integrated Personalized and Precision Oncology Network (IPPON), University of Antwerp, Antwerp, Belgium; [2]Department of Oncology, Antwerp University Hospital (UZA), Antwerp, Belgium; [3]Department of Pathology, Antwerp University Hospital (UZA), Antwerp, Belgium; [4]University of Groningen (RUG), European Research Institute for the Biology of Aging (ERIBA), University Medical Center Groningen (UMCG), Groningen, The Netherlands; [5]Department of Pulmonology and Thoracic Oncology, Antwerp University Hospital (UZA), Antwerp, Belgium; [6]Department of Thoracic and Vascular Surgery, Antwerp University Hospital (UZA), Antwerp, Belgium

Contributions: (I) Conception and design: A Domen, C Deben, I De Pauw, M Peeters, F Lardon, A Wouters; (II) Administrative support: C Deben, I De Pauw, M Peeters, F Lardon, A Wouters; (III) Provision of study materials or patients: M van de Wiel, A Janssens, JMH Hendriks, P Van Schil; (IV) Collection and assembly of data: C Hermans, H Lambrechts, V Siozopoulou, P Pauwels, M van de Wiel, A Janssens, JMH Hendriks, P Van Schil; (V) Data analysis and interpretation: A Domen, C Hermans, H Lambrechts, V Siozopoulou, P Pauwels, M Demaria, JB Vermorken, T Vandamme, H Prenen; (VI) Manuscript writing: All authors; (VII) Final approval of manuscript: All authors.

Correspondence to: Andreas Domen, MD. Center for Oncological Research (CORE), Integrated Personalized and Precision Oncology Network (IPPON), University of Antwerp, 2610 Antwerp, Belgium; Department of Oncology, Antwerp University Hospital (UZA), 2650 Antwerp, Belgium. Email: Andreas.Domen@uantwerpen.be.

Background: Cure and long-term survival for non-small cell lung cancer (NSCLC) remains hard to achieve. Cellular senescence, an emerging hallmark of cancer, is considered as an endogenous tumor suppressor mechanism. However, senescent cancer cells can paradoxically affect the surrounding tumor microenvironment (TME), ultimately leading to cancer relapse and metastasis. As such, the role of cellular senescence in cancer is highly controversial.

Methods: In 155 formalin-fixed paraffin-embedded (FFPE) samples from surgically resected NSCLC patients with pathological tumor-node-metastasis (pTNM) stages I–IV (8th edition), cellular senescence was assessed using a combination of four immunohistochemical senescence markers, i.e., lipofuscin, $p16^{INK4a}$, $p21^{WAF1/Cip1}$ and Ki67, and correlated to clinicopathological parameters and outcomes, including overall survival (OS) and disease-free survival (DFS).

Results: A tumoral senescence signature (SS) was present in 48 out of 155 NSCLC patients, but did not correlate to any clinicopathological parameter, except for *p53* mutation status. In a histologically homogenous patient cohort of 100 patients who fulfilled the following criteria: (I) one type of histology, i.e., adenocarcinoma, (II) without known epidermal growth factor receptor *(EGFR)* mutation, (III) curative (R0) resection and (IV) no neoadjuvant systemic therapy or radiotherapy, the median OS and DFS for patients with a tumoral SS (n=30, 30.0%) compared to patients without a tumoral SS (n=70, 70.0%) was 53 versus 141 months (P=0.005) and 45 versus 55 months (P=0.25), respectively. In multiple Cox proportional hazards

^ ORCID: Andreas Domen, 0000-0003-1398-3061; Christophe Deben, 0000-0001-8085-2040; Ines De Pauw, 0000-0003-2967-9611; Jasper Verswyvel, 0000-0002-6143-6436; Vasiliki Siozopoulou, 0000-0001-8608-4660; Patrick Pauwels, 0000-0002-8553-1921; Marco Demaria, 0000-0002-8429-4813; Annelies Janssens, 0000-0002-1464-163X; Jeroen M. H. Hendriks, 0000-0001-9145-3643; Paul Van Schil, 0000-0002-1962-8821; Jan B. Vermorken, 0000-0001-8515-7848; Timon Vandamme, 0000-0003-3701-5305; Hans Prenen, 0000-0001-8802-7352; Marc Peeters, 0000-0003-4969-2303; Filip Lardon, 0000-0001-7174-4144; An Wouters, 0000-0001-7771-1239.

(Cox PH) model analysis correcting for age, pTNM stage I–III and adjuvant therapy, a tumoral SS remained a significant prognostic factor for OS (HR =2.03; P=0.014).

Conclusions: The presence of a tumoral SS particularly based on high $p16^{INK4a}$ expression significantly affects OS in NSCLC adenocarcinoma. In this light, adjuvant senolytic therapy could be an interesting strategy for NSCLC patients harboring a tumoral SS, ultimately to improve survival of these patients.

Keywords: Senescence; survival; prognosis; non-small cell lung cancer (NSCLC)

Submitted Mar 15, 2022. Accepted for publication Jun 21, 2022.
doi: 10.21037/tlcr-22-192
View this article at: https://dx.doi.org/10.21037/tlcr-22-192

Introduction

Non-small cell lung cancer (NSCLC) remains a devastating disease and the leading cause of cancer-related death in men and women worldwide (1,2). Approximately 85% of all lung malignancies are classified as NSCLC (3), for which the predicted 5-year relative survival rate for newly diagnosed cases with squamous and adenocarcinoma histology is only 21.7% and 28.5%, respectively (4). Adenocarcinoma is the most common histological subtype accounting for >50% of cases (5) followed by squamous histology representing 25% to 30% of NSCLC (6).

Although surgery provides for most patients with NSCLC the pathway to cure and long-term survival (7), about 30% to 60% of patients with completely resected early-stage NSCLC will ultimately develop local, regional and/or distant recurrence or a second-primary lung cancer (8). Resectable locally advanced NSCLC is often treated with platinum-based chemotherapy in neoadjuvant or adjuvant setting, depending on mediastinal nodal involvement (9). However, recurrence rate of resected stage IIIA NSCLC in the first and second year is 41% and 36%, respectively (10). Hence, cure and long-term survival for NSCLC remains hard to achieve.

Cellular senescence, an emerging hallmark of cancer (11), is a durable and irreversible cell cycle arrest with secretory features, macromolecular damage and altered metabolism that is elicited in response to different stresses (12) {such as (I) DNA damage (i.e., DNA damage-induced senescence); (II) the activation of oncogenes (i.e., oncogene-induced senescence); (III) various anticancer drugs [i.e., therapy-induced senescence (TIS)] (13)} and that often activates a persistent DNA-damage response (14). Due to the induction of a durable and generally irreversible cell cycle arrest, cellular senescence is often considered as an endogenous tumor suppressor mechanism (11,13). However, senescent malignant and non-malignant cells stay metabolically active and can secrete a plethora of largely pro-inflammatory cytokines, chemokines, growth factors and matrix-remodeling proteases—collectively known as the senescence-associated secretory phenotype (SASP). This SASP protects malignant cells from immune clearance and affects the surrounding tumor microenvironment (TME), ultimately stimulating cancer relapse and metastasis (15,16). Also, the stability of the senescence-associated cell-cycle arrest might be hindered by the genomic instability intrinsic to malignant cells (12,17), thus producing more aggressive variants (18) and boosting the capacity to drive tumor growth (19,20). As such, the role of cellular senescence in cancer is ambiguous (11).

Identification and quantification of senescent cells is a challenging task since currently, there are no specific and universal markers for senescent cells (12,14). Also, the detection of senescence-associated beta-galactosidase (SA-β-Gal) activity and often considered as the gold standard for identifying cells, is only applicable in fresh snap-frozen tissue samples (21). Therefore, detection of cellular senescence in archival formalin-fixed paraffin-embedded (FFPE) samples should be achieved by combining the measurements of different markers for cellular senescence, as previously reported (12,14). As a result, *in vivo* and *ex vivo* evidence of cellular senescence in cancer patient samples is sparse and is only now catching up (12).

In this context, we assessed the clinical impact and significance of the presence of cellular senescence in NSCLC patients, treated with or without stage-dependent (neo)adjuvant therapy. Surgically resected FFPE samples were stained using a combination of four immunohistochemical senescence markers as previously described (12,14), i.e., lipofuscin aggregates, cell cycle inhibitors $p16^{INK4a}$ and $p21^{WAF1/Cip1}$ and proliferation marker

Ki67. Correlation with clinicopathological parameters and outcomes, including and overall survival (OS) and disease-free survival (DFS) was calculated. We present the following article in accordance with the STROBE reporting checklist (available at https://tlcr.amegroups.com/article/view/10.21037/tlcr-22-192/rc).

Methods

Patient and tissue sampling

Primary tumor specimens, including clinicopathological parameters, were obtained from 155 NSCLC patients with postsurgical pathological tumor-node-metastasis (pTNM) stage I–IV (8th edition), treated with or without stage-dependent (neo)adjuvant therapy, who underwent surgery at the Antwerp University Hospital (UZA) between 2007 and 2020, and were made available by the Biobank Antwerp (reference number BB19049), Antwerp, Belgium; ID: BE 71030031000 (22) of the UZA. The study was conducted in accordance with the Declaration of Helsinki (as revised in 2013) and was approved by the Ethics Committee of the Antwerp University Hospital (UZA) (reference number 19/18/236). Individual consent for this retrospective analysis was waived. OS was date of surgery until death by any cause. Patients without a date of death were censored at time of last follow-up. DFS was date of surgery until the first event of either recurrent disease or death.

Immunohistochemistry

FFPE tissue samples from 155 NSCLC patients were retrieved. Four separate, sequential and adjacent FFPE sections (5 µm thick) were cut using a HM340E microtome (Thermo Scientific®) and mounted on positively charged Superfrost Plus (Thermo Scientific®) slides that enable better adherence of the section, and stored at 4 ℃. Prior to staining, slides were placed in a 65 ℃ oven for 2 hours to melt the paraffin. Both positive and negative controls were included in all experiments.

Cellular senescence was assessed using a combination of four immunohistochemical senescence markers, i.e., lipofuscin aggregates, cell cycle inhibitor $p16^{INK4a}$ and $p21^{WAF1/Cip1}$ and proliferation marker Ki67, as previously described (12,14), as the detection of SA-β-Gal activity is only applicable in fresh snap-frozen tissue samples (21).

Lipofuscin staining

The first step involved deparaffinization by washing in xylene for 8 minutes and rehydration for 5 minutes through graded isopropanol solutions of 100%, 95%, 80%, 70% and 50%, respectively. Slides were then washed in wash solution [phosphate buffered saline (PBS) + 0.3% triton X-100] and incubated for 1 hour with 1% bovine serum albumin at room temperature to block non-specific binding of antibody. Next, the slides were washed in wash solution and incubated for 5 minutes with 3.5% H_2O_2 (Acros Organics®) at room temperature to block endogenous peroxidase activity. Slides were then washed in wash solution, followed by 5 minutes of incubation in 50% and 70% EtOH, respectively. Then, filtered (Millex-GP® syringe filter unit, a 33 mm diameter filter with 0.22 µm pore size) SenTraGor™ (Arriani pharmaceuticals®), a biotinylated Sudan Black B based chemical reagent, was applied on the slides and covered with a cover slip to avoid evaporation during the following incubation of 10 minutes at 37 ℃. Afterwards, the coverslip of each slide was removed gently, and the slides were washed in 50% EtOH for 5 minutes at room temperature. Next, the slides were washed in PBS + 0.5% triton X-100 for 3 minutes at room temperature to increase permeabilization, and then incubated for 1 hour at 37 ℃ with the anti-biotin primary antibody (Abcam®, Ab201341) at a dilution of 1/200 and covered with a cover slip to avoid evaporation. Afterwards, the coverslip of each slide was removed gently, the slides were washed in wash solution and incubated with EnVision Flex+ Mouse LINKER (Dako®) for 15 minutes at room temperature to amplify the signal of the primary antibody. The slides were then washed in wash solution and incubated with Envision Flex/HRP (Dako®) for 45 minutes at room temperature. After the incubation, slides were washed in wash solution and EnVision Flex HRP Magenta Substrate Chromogen/Substrate Buffer (Dako®) was applied for 5 minutes at room temperature. The slides were washed in wash solution and counterstained with hematoxylin for 1 minute. Finally, the slides were dehydrated for 1 minute in isopropanol solutions of 70%, 95% and 100%, respectively, cleared in xylene for 2 minutes and mounted with Quick-D mounting medium (Klinipath®). A positive and negative control was included in each staining run and consisted of liver tissue and replacement of SenTraGor™ reagent by PBS, respectively.

$p16^{INK4a}$, $p21^{WAF1/Cip1}$ and Ki67

The first step involved deparaffinization by washing in xylene for 8 minutes and rehydration for 5 minutes through graded isopropanol solutions of 100%, 95% and 70%, respectively, followed by 5 minutes in distilled

water. Subsequently, antigen retrieval with target retrieval solution—high pH (Dako®) in a PT Link pre-treatment module (Dako®) was conducted at pH 9.0 for 15 minutes ($p21^{WAF1/Cip1}$) or 20 minutes ($p16^{INK4a}$ and Ki67) at 97 ℃. Slides were washed for 5 minutes in Envision Flex Wash Buffer (Dako®) between each step. Endogenous peroxidase activity was quenched by incubating the slides in peroxidase blocking reagent for 5 minutes. Incubation with primary mouse monoclonal anti-human $p16^{INK4a}$ antibody (clone E6H4, ready to use, Roche Diagnostics®), $p21^{WAF1/Cip1}$ antibody (clone SX118, dilution 1/100, Agilent Technologies®) and Ki67 antibody (clone MIB-1, ready to use, Agilent Technologies®) was performed for 30, 40 and 20 minutes, respectively, at room temperature. Primary antibody incubation was followed by incubation with ready to use visualization reagent for 30 minutes ($p16^{INK4a}$) or mouse enhanced polymer-based linker (Mouse Linker, Dako®) for 15 minutes ($p21^{WAF1/Cip1}$ and Ki67). Detection and signal visualization was performed using visualization reagent (polymer reagent conjugated with horseradish peroxidase and affinity purified goat anti-mouse Fab' antibody fragments, supplied in stabilizing solution comprising preservatives and stabilizing protein, CINtec® Histology Kit) ($p16^{INK4a}$) or Envision FLEX/HRP (ready to use, 20 minutes, Dako®) ($p21^{WAF1/Cip1}$ and Ki67) followed by 10 minutes incubation with DAB Substrate-Chromogen solution (CINtec® Histology Kit) ($p16^{INK4a}$), and 5 minutes ($p21^{WAF1/Cip1}$) or 10 minutes (Ki67) incubation with the Dako Liquid DAB+ Substrate Chromogen System (Dako®). The slides were counterstained with hematoxylin for 2 minutes. Finally, the slides were dehydrated for 1 minute in isopropanol solutions of 70%, 95% and 100%, respectively, cleared in xylene for 2 minutes and mounted with Quick-D mounting medium (Klinipath®). A positive and negative control was included in each staining run and consisted for (I) $p16^{INK4a}$ respectively of tonsil tissue and replacement of primary mouse monoclonal anti-human $p16^{INK4a}$ antibody by Negative Reagent Control (Roche Diagnostics®), according to the manufacturer's instruction; for (II) $p21^{WAF1/Cip1}$ respectively of squamous cell lung carcinoma tissue and replacement of primary mouse monoclonal anti-human $p21^{WAF1/Cip1}$ antibody by FLEX Negative Control Mouse (Dako®), according to the manufacturer's instruction and for (III) Ki67 respectively of tonsil tissue and replacement of primary mouse monoclonal anti-human Ki67 antibody by FLEX Negative Control Mouse (Dako®), according to the manufacturer's instruction.

Assessment of immunohistochemical markers

Slides were scanned using an Ultra Fast (digital pathology slide scanner, Philips®) and images were analyzed using Image Management System viewer (pathology case viewer, Philips®). The percentage of tumor cells expressing the examined senescence markers was assessed in all optical ×200 fields available and the mean score was used to score each case. Lipofuscin accumulation, $p16^{INK4a}$ and $p21^{WAF1/Cip1}$ protein expression, and Ki67 expression were detected as cytoplasmic, mixed cytoplasmic/nuclear and nuclear stainings, respectively. Both an independent observer (AD) and a pathologist (VS) scored the different slides and scoring was performed blinded for clinical data.

A senescence signature (SS) was defined by the presence of high-level lipofuscin and high $p16^{INK4a}$ and/or $p21^{WAF1/Cip1}$ expression (≥30% NSCLC cells positive) in combination with low Ki67 expression (<30% NSCLC cells positive). An SS-p16 was defined by the presence of high-level lipofuscin and solely high $p16^{INK4a}$ expression (≥30% NSCLC cells positive) in combination with low Ki67 expression (<30% NSCLC cells positive). An SS-p21 was defined by the presence of high-level lipofuscin and solely high $p21^{WAF1/Cip1}$ expression (≥30% NSCLC cells positive) in combination with low Ki67 expression (<30% NSCLC cells positive). An SS-p16-p21 was defined by the presence of high-level lipofuscin and high $p16^{INK4a}$ and $p21^{WAF1/Cip1}$ expression (≥30% NSCLC cells positive) in combination with low Ki67 expression (<30% NSCLC cells positive).

Mutation analysis

Epidermal growth factor receptor (*EGFR*) and Kirsten rat sarcoma virus (*KRAS*) mutation status was determined as part of routine clinical practice by high-resolution melting analysis or next generation sequencing. *TP53* mutation status was determined in a subset of patients as previously described (23).

Statistical analysis

The statistical analysis was performed using IBM SPSS Statistics version 28.0. Correlation between individual senescence markers was analyzed using Spearman correlation. Association between SS and OS and DFS was studied using simple and multiple Cox proportional hazards (Cox PH) model to adjust for covariates (i.e., age, pTNM stage I–III and adjuvant therapy). Survival (OS) and

Table 1 Patient, tumor and treatment characteristics

Characteristic	Total cohort (n=155)	Homogenous cohort (n=100)
Age at diagnosis, years		
Mean (95% CI)	65 (64–66)	66 (64–68)
Median (min–max)	65 (39–85)	66 (45–85)
Gender, n (%)		
Female	58 (37.4)	40 (40.0)
Male	97 (62.6)	60 (60.0)
Smoking history, n (%)		
Positive	140 (90.3)	92 (92.0)
Negative	15 (9.7)	8 (8.0)
Histology, n (%)		
Adenocarcinoma	139 (89.7)	100 (100.0)
Squamous cell carcinoma	14 (9.0)	NA
Adenosquamous	1 (0.6)	NA
NOS	1 (0.6)	NA
Grade of differentiation, n (%)		
Well differentiated	50 (32.3)	40 (40.0)
Moderately differentiated	56 (36.1)	37 (37.0)
Poorly differentiated	49 (31.6)	23 (23.0)
Tumor size, cm, n (%)		
0–1.9	35 (22.6)	29 (29.0)
2–3.9	67 (43.2)	48 (48.0)
4–5.9	31 (20.0)	12 (12.0)
≥6	22 (14.2)	11 (11.0)
pTNM stage (8th edition), n (%)		
Stage I	67 (43.2)	54 (54.0)
Stage II	41 (26.5)	21 (21.0)
Stage III	39 (25.2)	25 (25.0)
Stage IV	8 (5.2)	NA
Surgical resection, n (%)		
R0	146 (94.2)	100 (100.0)
R1	9 (5.8)	NA
Mutation, positive/tested		
p53	19/53	12/36
EGFR	10/107	NA
KRAS	28/63	23/40
Treatment		
Neoadjuvant therapy, n (%)	39 (25.2)	NA
Cisplatin- or carboplatin-based doublet chemotherapy	36 (23.2)	NA
Cisplatin- or carboplatin-based doublet with radiotherapy	2 (1.3)	NA
Pembrolizumab with radiotherapy	1 (0.6)	NA
Surgery, n (%)	155 (100.0)	100 (100.0)
Adjuvant therapy, n (%)	46 (29.7)	27 (27.0)
Cisplatin- or carboplatin-based chemotherapy	29 (18.7)	21 (21.0)
Cisplatin- or carboplatin-based chemotherapy with radiotherapy	10 (6.5)	6 (6.0)
Radiotherapy only	7 (4.5)	NA

CI, confidence interval; NA, not applicable; NOS, not otherwise specified; pTNM, pathological tumor-node-metastasis; *EGFR*, epidermal growth factor receptor; *KRAS*, Kirsten rat sarcoma virus.

recurrence (DFS) curves were estimated using the Kaplan-Meier (KM) method. Differences between patients with and without an SS were studied using independent samples *t*-test or Mann-Whitney U test for continuous variables and Chi-square test or Fisher's exact test for categorical variables. P values <0.05 were considered to be statistically significant, and all tests were two-sided. Graphical presentation was performed using GraphPad Prism version 9.2.0.

Results

Presence of an SS, as assessed by immunohistochemical staining

The baseline patient, tumor and treatment characteristics of the total patient cohort and the homogenous patient cohort used for distribution analyses with clinicopathological parameters and survival analyses, respectively, are summarized in *Table 1*. The immunohistochemical expression of the four senescence markers in the total patient cohort and according to the tumoral SS status (i.e.,

Table 2 Expression of senescence markers in total cohort (n=155) and according to tumoral SS status

Senescence marker	Range	Median	Mean ± SD	High expression, n (%)	Low expression, n (%)	Negative expression, n (%)
% Lipofuscin + cells	0–100	50.0	46.9±30.5	103 (66.5)	52 (33.5)	8 (5.2)
SS (n=48)	30–100	67.5	65.3±19.7	48 (100.0)	0	0
No SS (n=107)	0–90	30.0	38.7±31.0	55 (51.4)	52 (48.6)	8 (7.5)
% $p16^{INK4a}$ + cells	0–100	30.0	38.5±38.3	78 (50.3)	77 (49.7)	41 (26.5)
SS (n=48)	0–100	62.5	58.8±33.8	39 (81.3)	9 (18.8)	5 (10.4)
No SS (n=107)	0–100	10.0	29.4±36.8	39 (36.4)	68 (63.6)	36 (33.6)
% $p21^{WAF1/Cip1}$ + cells	0–90	20.0	28.1±26.9	61 (39.4)	94 (60.6)	14 (9.0)
SS (n=48)	0–90	30.0	38.2±28.9	25 (52.1)	23 (47.9)	2 (4.2)
No SS (n=107)	0–90	15.0	23.5±24.8	36 (33.6)	71 (66.4)	12 (11.2)
% Ki67 + cells	0–95	17.5	28.2±25.4	60 (38.7)	95 (61.3)	3 (1.9)
SS (n=48)	0–28	8.3	10.2±7.9	0	48 (100.0)	2 (4.2)
No SS (n=107)	0–95	35.0	36.2±26.4	60 (56.1)	47 (43.9)	1 (0.9)

High expression: ≥30% NSCLC cells positive; low expression: <30% NSCLC cells positive. SS, senescence signature; SD, standard deviation; NSCLC, non-small cell lung cancer.

SS and no SS) is summarized in *Table 2*. *Figure 1* shows typical immunohistochemical correlation of high-level lipofuscin accumulation, high $p16^{INK4a}$ and $p21^{WAF1/Cip1}$ expression and low Ki67 expression, representing an SS. The presence of an SS was reported for 48 out of 155 NSCLC patients.

Correlation of individual senescence markers and according to tumoral SS status

First, we investigated whether the expression of the four individual senescence markers in the total patient cohort (n=155) and according to the tumoral SS status were correlated to each other to assess whether the individual senescence markers are interdependent for immunohistochemical detection of cellular senescence. Immunohistochemical $p16^{INK4a}$ expression, but not lipofuscin accumulation or $p21^{WAF1/Cip1}$ expression, was significantly inversely correlated with Ki67 expression (correlation coefficient =−0.32, P value <0.001). Immunohistochemical lipofuscin accumulation and $p21^{WAF1/Cip1}$ expression did not correlate to any of the individual senescence markers.

In patients with a tumoral SS (n=48), immunohistochemical $p16^{INK4a}$ expression was positively correlated with high-level lipofuscin accumulation (<30% NSCLC cells positive) (correlation coefficient =0.26, P value =0.071) and significantly inversely correlated with $p21^{WAF1/Cip1}$ expression (correlation coefficient =−0.34, P value =0.018). Conversely, in patients with no tumoral SS (n=107), immunohistochemical $p16^{INK4a}$ expression was significantly inversely correlated with lipofuscin accumulation (correlation coefficient =−0.24, P value =0.014) and significantly positively correlated with $p21^{WAF1/Cip1}$ expression (correlation coefficient =0.22, P value =0.024). Also, in patients with no tumoral SS, immunohistochemical Ki67 expression was significantly positively correlated with lipofuscin accumulation (correlation coefficient =0.33, P value <0.001) and significantly inversely correlated with $p16^{INK4a}$ expression (correlation coefficient =−0.22, P value =0.023).

Taken together, these results demonstrate an inverse correlation between immunohistochemical $p16^{INK4a}$ expression and Ki67 expression irrespective of an SS. According to the tumoral SS status, $p16^{INK4a}$ expression demonstrate differential correlations with lipofuscin accumulation and $p21^{WAF1/Cip1}$ expression.

Correlation of an SS with clinicopathological parameters

Next, we investigated whether the presence of an SS was associated with clinicopathological parameters in the total patient cohort of 155 patients. Presence of an SS was not

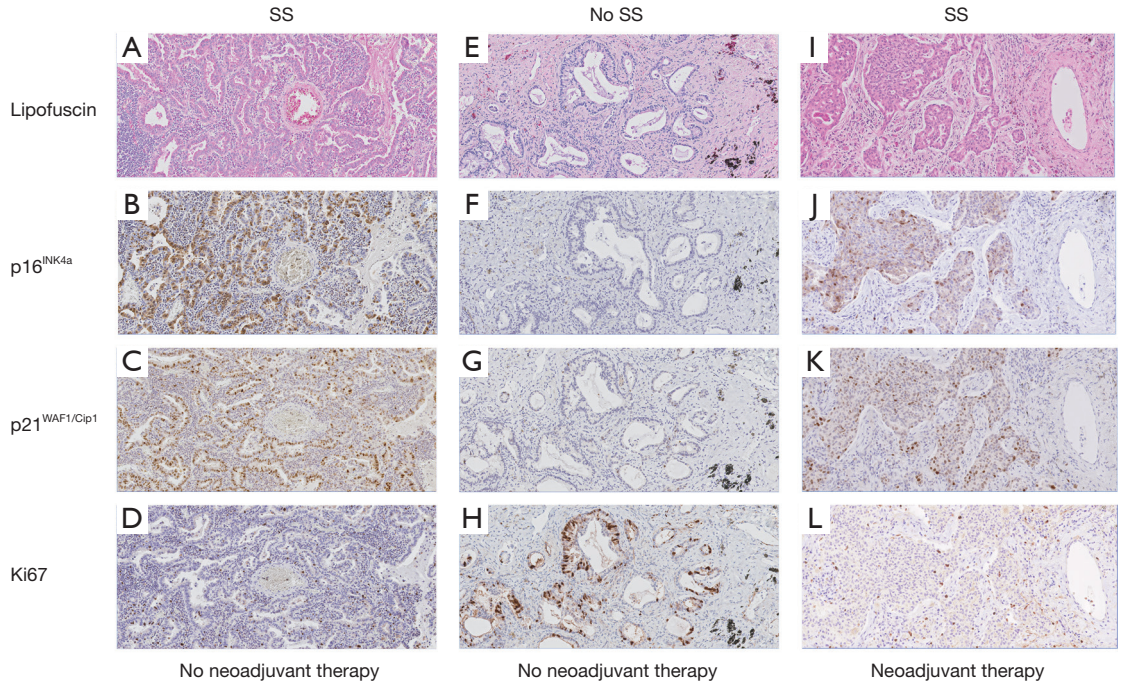

Figure 1 Immunohistochemical expression pattern of lipofuscin accumulation (A,E,I), $p16^{INK4a}$ (B,F,J), $p21^{WAF1/Cip1}$ (C,G,K) and Ki67 (D,H,L) at ×200 magnification on sequential and adjacent FFPE sections. Left and right panels represent stainings from two NSCLC patients with an SS with high-level lipofuscin accumulation (A,I), high $p16^{INK4a}$ (B,J) and $p21^{WAF1/Cip1}$ (C,K) expression (≥30% NSCLC cells positive) and low Ki67 expression (<30% NSCLC cells positive) (D,L). Left panels represent stainings from a NSCLC patient who did not receive any neoadjuvant therapy, whereas right panels represent stainings from a NSCLC patient who did receive neoadjuvant therapy (i.e., cisplatin-based chemotherapy). Middle panels represent stainings from a NSCLC patient showing no SS, with low-level lipofuscin accumulation (E), low $p16^{INK4a}$ (F) and $p21^{WAF1/Cip1}$ (G) expression (<30% NSCLC cells positive) and high Ki67 expression (≥30% NSCLC cells positive) (H). SS, senescence signature; FFPE, formalin-fixed paraffin-embedded; NSCLC, non-small cell lung cancer.

significantly associated with clinical parameters (age, gender and smoking history), pathological parameters (grade of differentiation, tumor size and pTNM stage) or *EGFR* and *KRAS* mutation status. However, an SS was significantly more present in case of confirmed *p53* wild-type samples compared to samples with a confirmed *p53* mutation (50.0% versus 21.1%, P=0.039).

As commonly used cancer interventions have been associated with the induction of cellular senescence (i.e., TIS) in cancer cells (16), we next analyzed the expression of the individual senescence markers as well as the presence of an SS according to neoadjuvant therapy. Patients who received neoadjuvant therapy showed a significantly higher mean lipofuscin accumulation (59.1% versus 42.8%, P=0.004) and Ki67 expression (37.4% versus 25.1%, P=0.015) compared to patients who did not receive any neoadjuvant treatment. $p16^{INK4a}$ (36.5% versus 39.2%, P=0.70) and $p21^{WAF1/Cip1}$ (29.6% versus 27.5%, P=0.68) expression were very comparable between patients with or without neoadjuvant therapy. Regarding the presence of an SS according to neoadjuvant therapy, an SS was not significantly more present in patients with neoadjuvant therapy compared to patients without neoadjuvant therapy (28.2% versus 31.9%, P=0.67). However, in case an SS was present, patients who did receive neoadjuvant therapy showed a higher mean lipofuscin accumulation (73.6% versus 62.7%, P=0.11) and a significantly higher $p16^{INK4a}$ expression (77.3% versus 53.4%, P=0.038) compared to patients without neoadjuvant therapy. $p21^{WAF1/Cip1}$ expression (39.1% versus 38.0%, P=0.91) and Ki67 expression (9.5% versus 10.4%, P=0.75) were very comparable between patients with or without neoadjuvant therapy.

In patients who did receive neoadjuvant therapy (n=39), an SS was more present in adenocarcinoma samples (9/24, 37.5%) compared to samples with another histological subtype (2/15, 13.3%). Also, within this subpopulation

of which the *p53* mutation status was determined (n=10), an SS was more present in *p53* wild-type samples (3/4, 75.0%) compared to samples which harbored a confirmed *p53* mutation (1/6, 16.7%). However, the analyses were performed in a small sample size and differences were non-significant.

Overall, these above-mentioned observations indicate that an SS is more present in *p53* wild-type samples, and neoadjuvant therapy might induce a new SS that is more pronounced or reinforce a pre-existing SS by increasing lipofuscin accumulation and $p16^{INK4a}$ expression.

Correlation between the presence of SS and survival

We next analyzed the relationship between the presence of an SS and OS in a histologically heterogenous patient cohort of 139 patients who had surgery with curative intent, i.e., excluding pTNM stage IV and resections with microscopically residual tumor (R1). With a median follow-up of 53 months, KM OS analysis showed a difference in median OS for patients with an SS compared to patients without an SS with a clear trend for worse OS for patients with an SS approaching significance (62 versus 88 months, P=0.059) (*Figure 2A*). Next, we selected a more histologically homogenous patient group consisting of 100 patients with pTNM stages I–III, according to the 8th edition, who fulfilled the following criteria: (I) one type of histology, i.e., adenocarcinoma, (II) without known *EGFR* mutation, (III) curative (R0) resection and (IV) no neoadjuvant systemic therapy or radiotherapy as neoadjuvant therapy is capable of inducing TIS (16) (*Table 1*). In this histologically homogenous patient cohort with a median follow-up of 57 months, KM OS analysis showed a significant difference in median OS for patients with an SS compared to patients without an SS (53 versus 141 months, P=0.005) (*Figure 2B*) with a 5-year OS rate of 44.9% versus 66.9%, respectively. The presence of an SS served as a significant prognostic factor for OS in simple [n=100; hazard ratio (HR) =2.17; P=0.007] and multiple (n=100; HR =2.03; P=0.014) Cox PH model analysis correcting for age, pTNM stage I–III and adjuvant therapy (*Table 3*). Interestingly, no individual senescence marker served as a significant prognostic factor for OS in simple and multiple Cox PH model analysis when scored as continuous or categorical [high (≥30% NSCLC cells positive)/low (<30% NSCLC cells positive) expression] variables. Regarding DFS, KM analysis showed difference in median DFS for patients with an SS compared to patients without an SS (45 versus 55 months) with a trend towards significance (P=0.25) (*Figure 2C*).

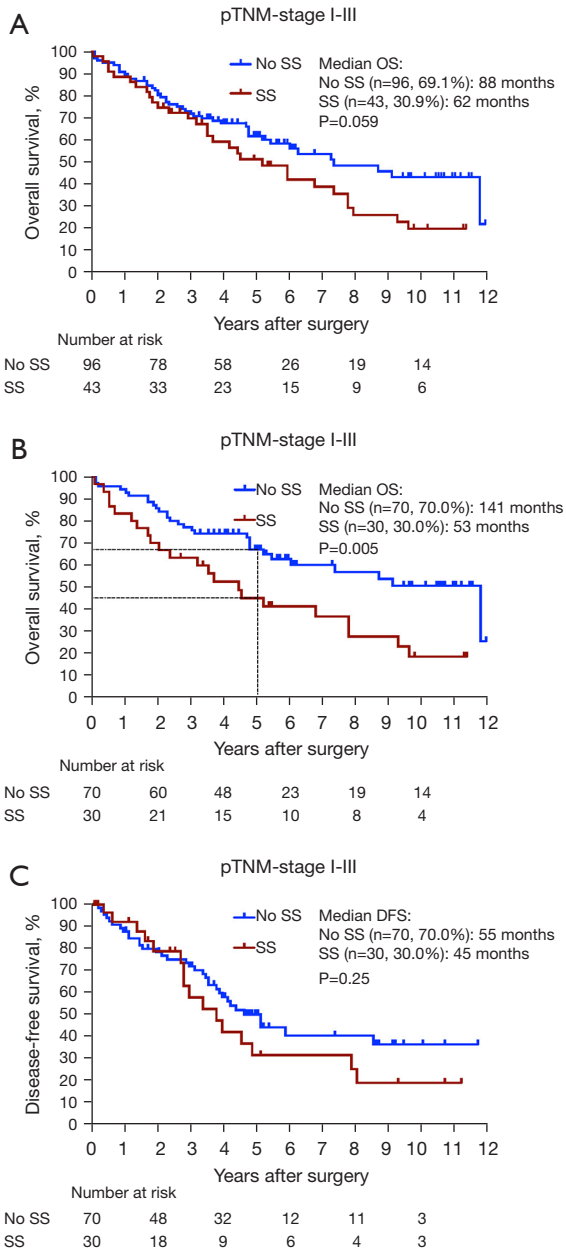

Figure 2 KM analysis for OS of 139 NSCLC patients with curative intent surgery (A), and for OS (B) and DFS (C) of a homogenous patient cohort of 100 patients with pTNM I–III according to SS. pTNM, pathological tumor-node-metastasis; SS, senescence signature; OS, overall survival; DFS, disease-free survival; KM, Kaplan-Meier; NSCLC, non-small cell lung cancer.

Collectively, these results demonstrate that the presence

Table 3 Prognostic value of an SS, SS-p16, SS-p21 and SS-p16-p21, as calculated with Cox PH model analysis

Characteristics	HR	95% CI	P value
Simple Cox PH model analysis			
SS	2.17	1.24–3.80	0.007*
SS-p16	2.23	1.05–4.73	0.037*
SS-p21	1.43	0.50–4.07	0.51
SS-p16-p21	2.74	1.29–5.81	0.009*
Multiple Cox PH model analysis correcting for age, pTNM stage I–III and adjuvant therapy			
SS	2.03	1.15–3.57	0.014*
SS-p16	2.10	0.97–4.53	0.059
SS-p21	1.31	0.46–3.79	0.61
SS-p16-p21	2.55	1.19–5.45	0.016*

*, HR is significant. Cox PH; Cox proportional hazards; HR, hazard ratio; CI, confidence interval; SS, senescence signature; pTNM, pathological tumor-node-metastasis.

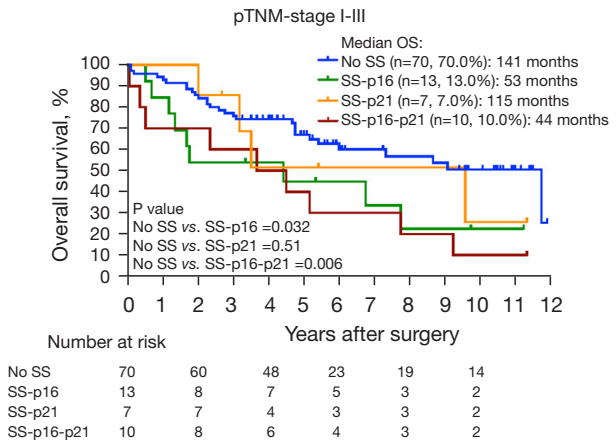

Figure 3 KM analysis for OS of a homogenous patient cohort of 100 NSCLC patients with pTNM I–III according to SS-p16, SS-p21 and SS-p16-p21. pTNM, pathological tumor-node-metastasis; SS, senescence signature; OS, overall survival; KM, Kaplan-Meier; NSCLC, non-small cell lung cancer.

of an SS has significant prognostic implications in resected NSCLC adenocarcinoma.

$p16^{INK4a}$ and $p21^{WAF1/Cip1}$ are both cell cycle inhibitor proteins, however, each capable of inducing senescence via different downstream pathways (24) and show independent immunohistochemical expression as mentioned above. Therefore, we determined the prognostic value of an SS defined by high-level lipofuscin plus low Ki67 expression, combined with (I) solely high $p16^{INK4a}$ expression (≥30% NSCLC cells positive, i.e., SS-p16); (II) solely high $p21^{WAF1/Cip1}$ expression (≥30% NSCLC cells positive, i.e., SS-p21); and (III) both high $p16^{INK4a}$ and high $p21^{WAF1/Cip1}$ (≥30% NSCLC cells positive, i.e., SS-p16-p21) expression. Compared to patients without any SS phenotype, KM OS analysis showed a worse OS for patients with an SS-p16 (53 versus 141 months, P=0.032) as well as for patients with an SS-p21 (115 versus 141 months, P=0.51), and patients with an SS-p16-p21 (44 versus 141 months, P=0.006) (*Figure 3*). The presence of an SS-p16 and an SS-p16-p21, but not an SS-p21, served as a significant prognostic factor for OS in simple Cox PH model analysis (*Table 3*). In multiple Cox PH model analysis correcting for age, pTNM stage I–III and adjuvant therapy, only the presence of an SS-p16-p21 remained as a significant prognostic factor whereas the presence of an SS-p16 and an SS-p21 did not (*Table 3* and *Figure 4*).

These results thus indicate that the presence of an SS particularly based on high $p16^{INK4a}$ expression has more profound impact on OS compared to an SS based on solely high $p21^{WAF1/Cip1}$ expression.

Discussion

Cellular senescence is considered as a protective mechanism, in addition to programmed cell death, for maintaining tissue homeostasis by inducing an irreversible proliferative arrest in dysfunctional and diseased cells (11), and has beneficial functions in a variety of physiological and pathological

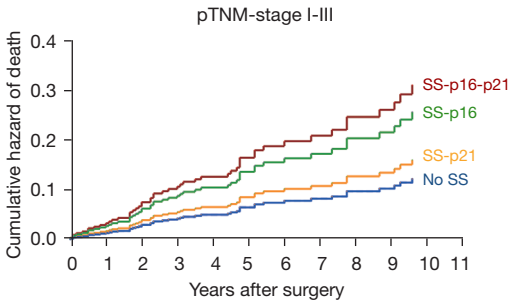

Figure 4 Cumulative risk of death in a homogenous patient cohort of 100 NSCLC patients with pTNM I–III according to SS-p16, SS-p21 and SS-p16-p21. pTNM, pathological tumor-node-metastasis; SS, senescence signature; NSCLC, non-small cell lung cancer.

processes, such as embryogenesis and wound healing (25). In cancer, cellular senescence has long been considered as an endogenous tumor suppressor mechanism by inducing senescence in pre- or fully malignant cells, thereby limiting malignant progression (11). However, despite the clear benefit of the senescence-associated growth arrest for preventing the expansion of pre- or fully malignant cells, senescent malignant (26) and non-malignant cells (27) are capable of paradoxically stimulating tumor relapse, progression and metastasis. This is presumably caused by the SASP as well as the genomic instability of malignant cells, overriding the senescence-associated cell cycle arrest over time (11).

Due to its importance in regulating various biological processes, and its ambiguous and even controversial role in cancer, *in vivo* evidence for cellular senescence in human tissue has gained more attention in the last decade (12). As a result, cellular senescence has recently been promoted as an emerging hallmark of cancer (11). However, little is known about the consequence of cellular senescence on prognosis and survival in distinct types of cancer. In breast cancer, high expression of a cellular senescence gene panel was associated with increased survival (28). In contrast, in hepatocellular carcinoma, a cellular senescence-associated gene signature in the TME was associated with worse DFS and OS (29). In prostate cancer, tumor-associated senescence has a dual role with tumor-suppressive as well as tumor-promoting properties, depending on deletion of the metalloproteinase inhibitor *TIMP1* (26).

In NSCLC, only two previous reports demonstrated a negative prognostic value of individual immunohistochemical senescence markers, such as lipofuscin accumulation (30) and high $p21^{WAF1/Cip1}$ and high Ki67 (31), however, both in rather histological heterogenous patient populations. On the contrary, loss of $p16^{INK4a}$ expression (<10%), which is a common feature especially in squamous cell carcinoma compared to adenocarcinoma (87% versus 50%, respectively), was associated with significantly worse OS (32). Nonetheless, to identify senescent cells with the highest accuracy, the International Cell Senescence Association (12) and Kohli *et al.* (14) recommend combining individual markers, as senescent cells lack specific and universal markers.

The present study demonstrates for the first time that the presence of a tumoral SS, based on the combination of four cellular senescence markers, negatively affects OS and DFS in NSCLC adenocarcinoma. In this context, senescent cancer cells could initially serve as a temporarily indolent cancer cell reservoir, with anti-apoptotic properties that evades immune clearance and molds a favorable surrounding TME by secreting SASP immunosuppressive cytokines and matrix-remodeling proteases. In later stages, the SASP can reinforce the senescent phenotype in an autocrine way, and paracrinally spread the senescent phenotype to adjacent malignant and non-malignant cells. With an increasing tumoral senescence burden, the accumulation of SASP can subsequently stimulate growth and proliferation of neighboring benign, premalignant and malignant cells (33). Finally, due to their genomic instability, and the possibility to acquire additional mutations that affect the function of cell-cycle arrest genes, senescent cancer cells can escape from the proliferative stall, probably resulting in loss of $p16^{INK4a}$ expression and compatible with previous findings of Sterlacci *et al.* (32), ultimately leading to disease recurrence and worse OS. The senescent phenotype spread by the tumoral SS to the adjacent non-tumoral tissue can contribute to the protumorigenic effects exhibited by the tumoral SS, ultimately promoting cancer relapse (27) (*Figure 5*). Of note, samples without a tumoral SS do not necessarily exclusively harbor non-senescent proliferating cancer cells but nevertheless can also harbor few senescent cancer cells. Since senescence is considered antagonistically pleiotropic (34), it could be suggested that the quantity of senescent cancer cells in these samples is not sufficient to exhibit similar protumorigenic effects as in samples with a high tumoral senescence burden, and the occasional senescent cells act primarily tumor suppressive through the senescent-associated cell cycle arrest. The relationship between the presence of a tumoral SS and DFS was less

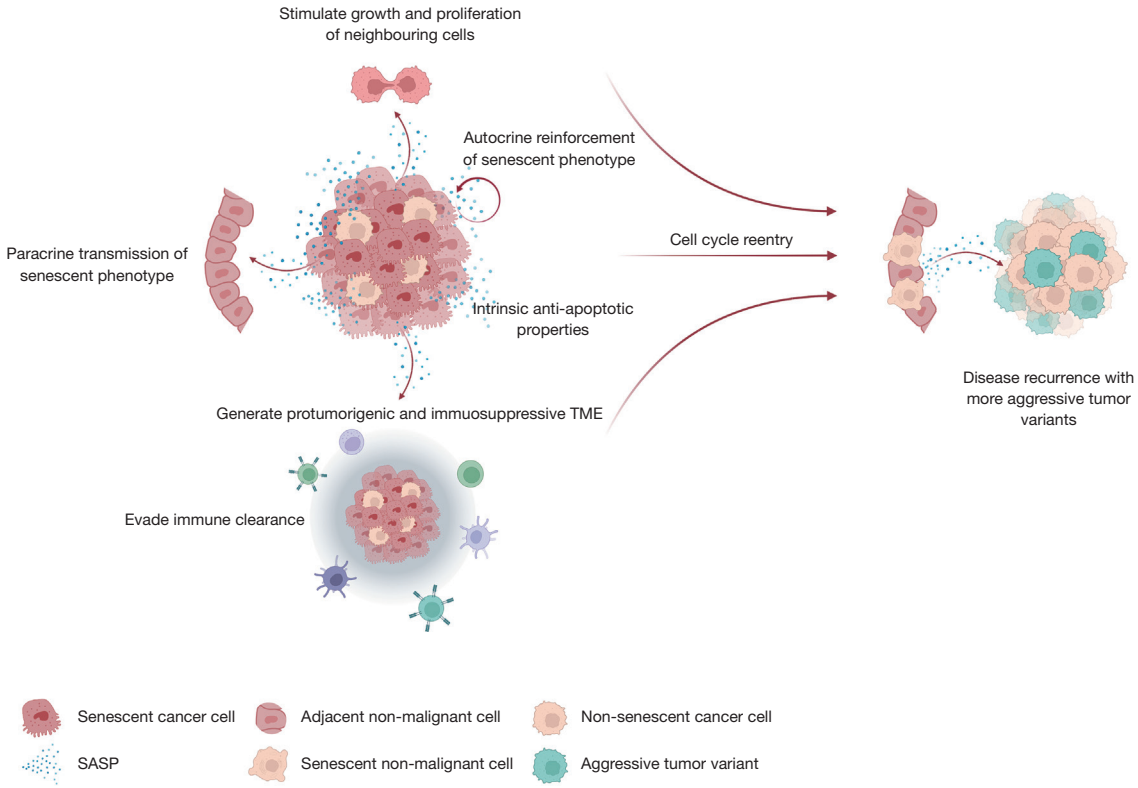

Figure 5 Schematic representation of potential mechanism behind tumoral SS in NSCLC. TME, tumor microenvironment; SASP, senescence-associated secretory phenotype; SS, senescence signature; NSCLC, non-small cell lung cancer.

clear. Possibly, a tumoral SS does not necessarily result in a shorter DFS but rather, in case of disease recurrence, results in a more aggressive disease course due to more aggressive tumor variants produced by the tumoral SS (*Figure 5*). However, since the retrospective nature of the study, DFS was not an ideal primary endpoint.

Interestingly, Lin *et al.* (35) recently demonstrated that NSCLC adenocarcinoma patients with a highly expressed senescence-related gene signature experienced a significantly shorter OS compared to patients with low expression of these senescence-related genes, confirming our results, however, at transcriptional level.

Cellular senescence is predominantly regulated by the activation of cell cycle inhibitors $p21^{WAF1/Cip1}$ and/or $p16^{INK4a}$, as most senescence-inducing stresses leads to the activation of the cell cycle inhibitor pathways $p53/p21^{WAF1/Cip1}$ and/or $p16^{INK4a}$ (24). Activation $p21^{WAF1/Cip1}$ and/or $p16^{INK4a}$ will induce a stable cell cycle arrest by inhibition of cyclin-dependent kinase 1 (CDK1), CDK2, CDK4 and CDK6 and thereby prevents phosphorylation of the retinoblastoma protein (24), a tumor suppressor protein blocking S-phase entry (36). However, $p21^{WAF1/Cip1}$ expression occurs earlier after senescence induction and is reversible upon tumor suppressor protein p53 inactivation, in contrast to $p16^{INK4a}$ that is frequently expressed late after senescence induction and irreversible upon p53 inactivation (14,37,38). As such, $p53/p21^{WAF1/Cip1}$ pathway activation seems to be more involved in the initiation of senescence, while $p16^{INK4a}$ seem to be more crucial for maintaining the senescence-associated arrest (38). Interestingly, our data shows that an SS based on solely $p16^{INK4a}$ expression (i.e., SS-p16) and an SS based on high expression of both $p16^{INK4a}$ and high $p21^{WAF1/Cip1}$ (i.e., SS-p16-p21) had a more profound impact on OS in contrast to an SS based on solely high $p21^{WAF1/Cip1}$ expression (i.e., SS-p21). Possibly, an SS based on high $p16^{INK4a}$ expression is more durable and therefore more protumorigenic with established SASP production compared to a premature SS based on solely high $p21^{WAF1/Cip1}$ expression.

Although cell cycle inhibitor pathways $p53/p21^{WAF1/Cip1}$ and $p16^{INK4a}$ are intertwined, DNA-damage, oncogene activation and tumor suppressor inactivation mainly lead to the activation of tumor suppressor protein p53 and

consequently $p21^{WAF1/Cip1}$ through the Ras-Raf-MEK-ERK or AKT signaling pathways (24). In accordance, an SS was more present in *p53* wild-type samples compared to *p53* mutated samples, where induction of senescence via p53/$p21^{WAF1/Cip1}$ pathway activation is presumably defective (23). Nonetheless, cellular senescence can also be induced through activation of $p16^{INK4a}$, irrespective of p53/$p21^{WAF1/Cip1}$ pathway activation (24).

Regarding TIS, an SS was not more present in patients who received neoadjuvant therapy compared to patients who did not receive any neoadjuvant therapy. However, the SS in patients who received neoadjuvant therapy was more pronounced based on the lipofuscin accumulation and $p16^{INK4a}$ expression, suggesting stronger induction of a new SS or reinforcement of a pre-existing SS by neoadjuvant therapy. Also, neoadjuvant therapy was more prone to induce an SS in adenocarcinoma and *p53* wild-type samples compared to samples with other histology or *p53* mutation. However, the results of these sub-analyses were non-significant and need to be interpreted with caution due to the small sample size.

This study has several limitations. The data represent a retrospective review of a cohort of patients seen at a single academic institution over a period of 14 years, and not all patients received their follow-up at our center. Therefore, OS was used as a primary endpoint.

Another limitation of the study, as mentioned above, is the sample size. However, even in this small population of NSCLC patients, significant differences in survival analyses were seen, suggesting that the presence of an SS could have a profound impact on OS. Nonetheless, our preliminary results need to be confirmed in a large-scale population and prospective study design.

In the future, we plan to enlarge our sample size and include more NSCLC patients with histological subtypes other than adenocarcinoma to better delineate the differences that could exist within histology and within *EGFR* and *KRAS* mutation status.

In conclusion, the presence of an SS particularly based on high $p16^{INK4a}$ expression was significantly negatively associated with OS in NSCLC adenocarcinoma after correction for age, pTNM stage and adjuvant therapy. Since senolytics (i.e., compounds that selectively target senescent cells) are currently being evaluated in clinical trials for age-related pathologies such as osteoarthritis (NCT04815902) and Alzheimer's disease (NCT04063124) and are proposed as a novel cancer therapy (16,39-41), we suggest that adjuvant senolytic therapy could be an interesting strategy for NSCLC adenocarcinoma patients harboring an SS, ultimately to improve survival of these patients.

Acknowledgments

We thank Kristien Wouters [UZA, Edegem (Antwerp), Belgium] for assisting the statistical analyses.

This research was funded by donations from different donors, including Dedert Schilde vzw and Willy Floren.

Figure 5 was created with Biorender.com.

Funding: This work was supported by the University Research Fund (BOF) of the University of Antwerp, Antwerp, Belgium (No. FFB180188 to AD).

Footnote

Reporting Checklist: The authors have completed the STROBE reporting checklist. Available at https://tlcr.amegroups.com/article/view/10.21037/tlcr-22-192/rc

Data Sharing Statement: Available at https://tlcr.amegroups.com/article/view/10.21037/tlcr-22-192/dss

Peer Review File: Available at https://tlcr.amegroups.com/article/view/10.21037/tlcr-22-192/prf

Conflicts of Interest: All authors have completed the ICMJE uniform disclosure form (available at https://tlcr.amegroups.com/article/view/10.21037/tlcr-22-192/coif). The authors have no conflicts of interest to declare.

Ethical Statement: The authors are accountable for all aspects of the work in ensuring that questions related to the accuracy or integrity of any part of the work are appropriately investigated and resolved. The study was conducted in accordance with the Declaration of Helsinki (as revised in 2013) and was approved by the Ethics Committee of the Antwerp University Hospital (UZA) (reference number 19/18/236). Individual consent for this retrospective analysis was waived.

References

1. Planchard D, Popat S, Kerr K, et al. Metastatic non-small cell lung cancer: ESMO Clinical Practice Guidelines for diagnosis, treatment and follow-up. Ann Oncol 2018;29:iv192-237.
2. Siegel RL, Miller KD, Jemal A. Cancer statistics, 2018. CA Cancer J Clin 2018;68:7-30.
3. Herbst RS, Morgensztern D, Boshoff C. The biology and management of non-small cell lung cancer. Nature 2018;553:446-54.
4. Howlader N, Noone AM, Krapcho M, et al. Lung and Bronchus SEER 5-Year Relative Survival Rates, 2011-2017. Available online: https://seer.cancer.gov/explorer/application.html?site=47&data_type=4&graph_type=5&compareBy=subtype&chk_subtype_612=612&chk_subtype_613=613&chk_subtype_611=611&chk_subtype_610=610&series=9&sex=1&race=1&age_range=1&stage=101&advopt_precision=1&advopt_show_ci=on&advopt_display=2
5. Girard N, Sima CS, Jackman DM, et al. Nomogram to predict the presence of EGFR activating mutation in lung adenocarcinoma. European Respiratory Journal 2012;39:366-72.
6. Socinski MA, Obasaju C, Gandara D, et al. Clinicopathologic Features of Advanced Squamous NSCLC. J Thorac Oncol 2016;11:1411-22.
7. Osarogiagbon RU, Veronesi G, Fang W, et al. Early-Stage NSCLC: Advances in Thoracic Oncology 2018. J Thorac Oncol 2019;14:968-78.
8. Conforti F, Pala L, Pagan E, et al. Effectiveness of intensive clinical and radiological follow-up in patients with surgically resected NSCLC. Analysis of 2661 patients from the prospective MAGRIT trial. Eur J Cancer 2020;125:94-103.
9. Postmus PE, Kerr KM, Oudkerk M, et al. Early and locally advanced non-small-cell lung cancer (NSCLC): ESMO Clinical Practice Guidelines for diagnosis, treatment and follow-up. Ann Oncol 2017;28:iv1-21.
10. Lou F, Sima CS, Rusch VW, et al. Differences in patterns of recurrence in early-stage versus locally advanced non-small cell lung cancer. Ann Thorac Surg 2014;98:1755-60; discussion 1760-1.
11. Hanahan D. Hallmarks of Cancer: New Dimensions. Cancer Discov 2022;12:31-46.
12. Gorgoulis V, Adams PD, Alimonti A, et al. Cellular Senescence: Defining a Path Forward. Cell 2019;179:813-27.
13. Hernandez-Segura A, Nehme J, Demaria M. Hallmarks of Cellular Senescence. Trends Cell Biol 2018;28:436-53.
14. Kohli J, Wang B, Brandenburg SM, et al. Algorithmic assessment of cellular senescence in experimental and clinical specimens. Nat Protoc 2021;16:2471-98.
15. Faget DV, Ren Q, Stewart SA. Unmasking senescence: context-dependent effects of SASP in cancer. Nat Rev Cancer 2019;19:439-53.
16. Wang B, Kohli J, Demaria M. Senescent Cells in Cancer Therapy: Friends or Foes? Trends Cancer 2020;6:838-57.
17. Roberson RS, Kussick SJ, Vallieres E, et al. Escape from therapy-induced accelerated cellular senescence in p53-null lung cancer cells and in human lung cancers. Cancer Res 2005;65:2795-803.
18. Yang L, Fang J, Chen J. Tumor cell senescence response produces aggressive variants. Cell Death Discov 2017;3:17049.
19. Medema JP. Escape from senescence boosts tumour growth. Nature 2018;553:37-8.
20. Milanovic M, Fan DNY, Belenki D, et al. Senescence-associated reprogramming promotes cancer stemness. Nature 2018;553:96-100.
21. Evangelou K, Lougiakis N, Rizou SV, et al. Robust, universal biomarker assay to detect senescent cells in biological specimens. Aging Cell 2017;16:192-7.
22. BE 71030031000; Biobank Antwerp [BB19049], BBMRI-ERIC, Belgian [BIORESOURCE].
23. Deben C, Deschoolmeester V, Lardon F, et al. TP53 and MDM2 genetic alterations in non-small cell lung cancer: Evaluating their prognostic and predictive value. Crit Rev Oncol Hematol 2016;99:63-73.
24. Paez-Ribes M, González-Gualda E, Doherty GJ, et al. Targeting senescent cells in translational medicine. EMBO Mol Med 2019;11:e10234.
25. He S, Sharpless NE. Senescence in Health and Disease. Cell 2017;169:1000-11.
26. Guccini I, Revandkar A, D'Ambrosio M, et al. Senescence Reprogramming by TIMP1 Deficiency Promotes Prostate Cancer Metastasis. Cancer Cell 2021;39:68-82.e9.
27. Demaria M, O'Leary MN, Chang J, et al. Cellular Senescence Promotes Adverse Effects of Chemotherapy and Cancer Relapse. Cancer Discov 2017;7:165-76.
28. Althubiti M, Lezina L, Carrera S, et al. Characterization of novel markers of senescence and their prognostic potential in cancer. Cell Death Dis 2014;5:e1528.

29. Eggert T, Wolter K, Ji J, et al. Distinct Functions of Senescence-Associated Immune Responses in Liver Tumor Surveillance and Tumor Progression. Cancer Cell 2016;30:533-47.
30. Giatromanolaki A, Kouroupi M, Balaska K, et al. A Novel Lipofuscin-detecting Marker of Senescence Relates With Hypoxia, Dysregulated Autophagy and With Poor Prognosis in Non-small-cell-lung Cancer. In Vivo 2020;34:3187-93.
31. Dosaka-Akita H, Hommura F, Mishina T, et al. A risk-stratification model of non-small cell lung cancers using cyclin E, Ki-67, and ras p21: different roles of G1 cyclins in cell proliferation and prognosis. Cancer Res 2001;61:2500-4.
32. Sterlacci W, Tzankov A, Veits L, et al. A comprehensive analysis of p16 expression, gene status, and promoter hypermethylation in surgically resected non-small cell lung carcinomas. J Thorac Oncol 2011;6:1649-57.
33. Gonzalez-Meljem JM, Apps JR, Fraser HC, et al. Paracrine roles of cellular senescence in promoting tumourigenesis. Br J Cancer 2018;118:1283-8.
34. Campisi J. Aging, tumor suppression and cancer: high wire-act! Mech Ageing Dev 2005;126:51-8.
35. Lin W, Wang X, Wang Z, et al. Comprehensive Analysis Uncovers Prognostic and Immunogenic Characteristics of Cellular Senescence for Lung Adenocarcinoma. Front Cell Dev Biol 2021;9:780461.
36. Giacinti C, Giordano A. RB and cell cycle progression. Oncogene 2006;25:5220-7.
37. Alcorta DA, Xiong Y, Phelps D, et al. Involvement of the cyclin-dependent kinase inhibitor p16 (INK4a) in replicative senescence of normal human fibroblasts. Proc Natl Acad Sci U S A 1996;93:13742-7.
38. Beauséjour CM, Krtolica A, Galimi F, et al. Reversal of human cellular senescence: roles of the p53 and p16 pathways. EMBO J 2003;22:4212-22.
39. van Deursen JM. Senolytic therapies for healthy longevity. Science 2019;364:636-7.
40. Sieben CJ, Sturmlechner I, van de Sluis B, et al. Two-Step Senescence-Focused Cancer Therapies. Trends Cell Biol 2018;28:723-37.
41. Lee S, Schmitt CA. The dynamic nature of senescence in cancer. Nat Cell Biol 2019;21:94-101.

Cite this article as: Domen A, Deben C, De Pauw I, Hermans C, Lambrechts H, Verswyvel J, Siozopoulou V, Pauwels P, Demaria M, van de Wiel M, Janssens A, Hendriks JMH, Van Schil P, Vermorken JB, Vandamme T, Prenen H, Peeters M, Lardon F, Wouters A. Prognostic implications of cellular senescence in resected non-small cell lung cancer. Transl Lung Cancer Res 2022;11(8):1526-1539. doi: 10.21037/tlcr-22-192